

Magnetic white dwarfs with debris discs

B. Külebi^{1,2*}, K.Y. Ekşi^{3†}, P. Lorén–Aguilar⁴, J. Isern^{1,2} and E. García–Berro^{2,5}

¹ *Institut de Ciències de l’Espai (CSIC), Facultat de Ciències, Campus UAB, Torre C5-parell, 08193 Bellaterra, Spain*

² *Institute for Space Studies of Catalonia, c/Gran Capità 2–4, Edif. Nexus 104, 08034 Barcelona, Spain*

³ *Istanbul Technical University, Faculty of Science and Letters, Physics Engineering Department, Maslak 34469, Istanbul, Turkey*

⁴ *University of Exeter, School of Physics, Stocker Road, Exeter EX4 4QL, United Kingdom*

⁵ *Departament de Física Aplicada, Universitat Politècnica de Catalunya, c/Esteve Terrades, 5, 08860 Castelldefels, Spain*

29 September 2018

ABSTRACT

It has long been accepted that a possible mechanism for explaining the existence of magnetic white dwarfs is the merger of a binary white dwarf system, as there are viable mechanisms for producing sustainable magnetic fields within the merger product. However, the lack of rapid rotators in the magnetic white dwarf population has been always considered a problematic issue of this scenario. Smoothed Particle Hydrodynamics simulations show that in mergers in which the two white dwarfs have different masses a disc around the central compact object is formed. If the central object is magnetized it can interact with the disc through its magnetosphere. The torque applied by the disc changes the spin of the star, whereas the transferred angular momentum from the star to the disc determines the properties of the disc. In this work we build a model for the disc evolution under the effect of magnetic accretion, and for the angular momentum evolution of the star, which can be compared with the observations. Our model predicts that the magnetospheric interaction of magnetic white dwarfs with their discs results in a significant spin down, and we show that for magnetic white dwarfs with relatively strong fields (larger than 10 MG) the observed rotation periods of the magnetic white dwarf population can be reproduced. We also investigate whether turbulence can be sustained during the late phases of the evolution of the system. When a critical temperature below which turbulence is not sustained is introduced into the model, the periods of the three fast rotating, strongly magnetic, massive white dwarfs in the solar neighborhood are recovered.

Key words: stars: white dwarfs, stars: magnetic field, accretion discs

1 INTRODUCTION

Magnetic white dwarfs (MWDs) — white dwarfs with field strengths ranging from about 1 kG (Jordan et al. 2007) up to approximately 1 GG (Kawka et al. 2007; Külebi et al. 2009) — comprise more than about 10% of all white dwarfs. There are two possibilities to account for the observed magnetic fields. According to the fossil field hypothesis, these white dwarfs descend from Ap/Bp stars (Angel et al. 1981), and their magnetic fields are remnants of the previous evolution. One of the key properties of the population of MWDs is their mass distribution, since it turns out that their average mass is considerably larger than that of the field population (Kawka et al. 2007). Moreover, the reverse is also true, and the incidence of magnetism is larger in the population

of massive white dwarfs (Vennes & Kawka 2008). Within the framework of the fossil field hypothesis this has been explained as a result of the average higher mass of the magnetic progenitor systems Ap/Bp. However, detailed population synthesis studies show that the observed number of Ap/Bp stars is insufficient to explain the number of MWDs, and the contribution of an unseen population of weakly magnetized A/B stars needs to be invoked (Wickramasinghe & Ferrario 2005). The second possibility is that high-field MWDs are produced in the aftermath of the merger of two initially less massive white dwarfs. This scenario has been suggested as a viable mechanism for producing ultra-massive white dwarfs ($M_{\text{WD}} > 1.1 M_{\odot}$), and naturally explains why MWDs are more massive than their field counterparts. This scenario was first invoked for addressing the hot and massive population of white dwarfs in the ROSAT survey (Marsh et al. 1997), and recently to account for the high mass peak in the white dwarf mass distribution

* E-mail: kulebi@ice.cat

† E-mail: ekxi@itu.edu.tr

(Kepler et al. 2007). Since the incidence of magnetism is higher for this population of ultra-massive white dwarfs (Wickramasinghe & Ferrario 2000), the merger scenario provides a natural explanation for the properties of several MWDs, REJ 0317–853 (Barstow et al. 1995; Ferrario et al. 1997; Vennes et al. 2003) and SDSS J150746.80+520958.0 (Dobbie et al. 2011) being some representative examples.

There have been numerous suggestions that binary evolution could be responsible for magnetism in white dwarfs. Specifically, Tout et al. (2008) and Nordhaus et al. (2011) discussed the possibility that turbulence during a common envelope phase could generate strong magnetic fields. These studies were aimed at explaining two observational facts. The first one is that no high-field MWDs have been detected in detached binary systems with M dwarfs (Liebert et al. 2005), while the second one is the higher incidence of magnetism in white dwarfs in cataclysmic variables (approximately 25%) with respect to that of single stars (approximately 10%) — see, for instance, Warner (1995). All these motivated Tout et al. (2008) to put forward the hypothesis that magnetism is a direct consequence of binarity, and specifically of the evolution during the common envelope phase of a close binary system. Specifically, Tout et al. (2008) argued that isolated MWDs have merged, whereas those in magnetic cataclysmic variables have not. They therefore argued that the fields must have been generated before the merger, during the common envelope phase. Following the merger there would be a period of normal red giant evolution in which the star would spin down until the magnetized core would emerge as a slowly rotating MWD. Only when the merger occurs just when the envelope is ejected would the white dwarf emerge rapidly rotating. However, a few years later Potter & Tout (2010) showed that the magnetic fields generated in this way are not durable if only simple diffusion of the field into the degenerate white dwarf matter is considered, because of the long associated time scales.

There are other processes that might produce magnetic fields during binary evolution. One of such process is the effect of shear during the intense accretion phase before ignition in an accreting white dwarf, and also during the carbon simmering phase after the ignition (Piro 2008). By using the physical reasoning of Piro & Bildsten (2007), Piro (2008) proposed that poloidal and toroidal fields are produced due to a Taylor-Spruit dynamo during the differentially rotating phase. Their calculations show that for a white dwarf with $M_{\text{WD}} = 1.37 M_{\odot}$, $\Omega_{\text{WD}} = 0.1\Omega_{\text{K}} = 0.67 \text{ s}^{-1}$, $\dot{M} = 10^{-7} M_{\odot} \text{ yr}^{-1}$ — where Ω_{K} is the Keplerian velocity — the shear layer produces a magnetic field with components $B_{\phi} \approx 10^8 \text{ G}$ and $B_r \approx 10^5 \text{ G}$.

The merger of two white dwarfs has become an active area of research during the last years. This is mostly due to the belief that double degenerate mergers might be successful progenitors of Type Ia supernovae. Although this hypothesis is relatively old (Iben & Tutukov 1984; Webbink 1984), this scenario has recently received a vigorous interest — see, for instance, Bloom et al. (2012) and Schaefer & Pagnotta (2012). Other reasons of interest in these models are the possibilities that white dwarf mergers could form magnetars (King et al. 2001; Levan et al. 2006) and the detection of dust discs around white dwarfs (Kilic & Redfield 2007; García-Berro et al.

2007; von Hippel et al. 2007; Gänsicke et al. 2007, 2008; Brinkworth et al. 2009) and dust discs around MWDs (Reid et al. 2001; Dufour et al. 2006; Farihi et al. 2011; Kawka & Vennes 2011) which might be indicative of a former viscous disc phase following a merger process.

In essence, modern hydrodynamical simulations of the merger of two white dwarfs show that the less massive secondary is totally disrupted. Depending on the mass ratio of the binary components this process occurs on a dynamical time scale. As a result of the disruption of the secondary, part of its material is accreted on the primary, whereas the rest of it forms a rapidly rotating Keplerian disc. This confirms the early suggestions (Tutukov & Yungelson 1979; Nomoto & Iben 1985) that a thick disc should be produced as an intermediary step following the coalescence in which high accretion rates could be avoided and a SNIa explosion could take place. All these hypotheses have been recently confirmed by the in-depth SPH simulations of Guerrero et al. (2004), Yoon et al. (2007), Lorén-Aguilar et al. (2009), and Dan et al. (2012). In particular, all these simulations show that a thermally supported shock heated region forms around the central object (the undisturbed primary) and, additionally, they also predict the formation of a massive thick disc supported by Keplerian rotation.

The accretion phase after the initial violent merger phase has also been subsequently investigated. Recent calculations of the long-term evolution of the merger (Piersanti et al. 2003b,a; Yoon et al. 2007; van Kerkwijk et al. 2010) show that a supernova explosion is a likely outcome, although in the case of off-centre carbon ignition the result could also be an accretion induced collapse (AIC) to form a neutron star (Nomoto & Iben 1985). However, there are multiple processes that influence the long-term evolution of the merger product. One of these is the interaction of the white dwarf with the thin disc. Recently, Saio & Nomoto (2004) studied this interaction through the viscous boundary layer relying on the models of Paczynski (1991) and Popham & Narayan (1991). The current understanding is that an initial accretion stage nearly at the Eddington rate (about $10^{-5} M_{\odot} \text{ yr}^{-1}$) is unavoidable. More recently, another model has been proposed in which the thick disc evolves towards a spherical, thermally supported envelope due to the shear induced by the differential rotation within a short timescale of 10^4 s (Shen et al. 2012; Schwab et al. 2012). In both scenarios, the formation of ONE white dwarfs or, depending on the total mass of the system, of neutron stars via AIC, are the expected results.

Finally, García-Berro et al. (2012) proposed that the magnetic fields are generated in the corona above the merger product through an $\alpha\omega$ dynamo, since convection and differential rotation exist simultaneously. Using the results of the simulations of Lorén-Aguilar et al. (2009) they showed that very large magnetic fields can be generated in the hot corona resulting from a merger. Moreover, these magnetic fields do not diffuse into the white dwarf core or the surrounding disc, and remain confined to the outer layers, with strengths comparable to those observed in MWDs. This finding has been recently corroborated by Schwab et al. (2012) using the Høiland criterion. All in all, this means that magnetic fields can be naturally produced in the merger of two

white dwarfs. However, one problem of this scenario is the excess of the remnant angular momentum, that is incompatible with observations of MWDs. García-Berro et al. (2012) suggested magneto-dipole radiation as a possible solution for this drawback of the model. However, it is likely that magneto-dipole radiation would not be efficient enough to slow down the remnants of the coalescence to the observed rotation periods of MWDs. Nevertheless, if the merger product has high magnetic dipole fields and the disc from the merger survives, it is possible that the long-term evolution of the system will involve angular momentum exchange between the disc and the star, depending on the magnetic field strength of the central object.

In this paper we analyse the long-term evolution of the disc and of the central object resulting from the coalescence of two white dwarfs, carrying over some elements from models (Chatterjee et al. 2000; Alpar 2001; Ertan et al. 2009) constructed for supernova fallback discs around young neutron stars (Wang et al. 2006). Our paper is organized as follows. In Sect. 2 we explain the details of our model for the debris disc plus MWD system, in Sect. 3 we use the results of the SPH simulations of Lorén-Aguilar et al. (2009) and the fallback model presented in Sect. 2 to compare our simulations with the observations of MWDs. Finally, in Sect. 4, we summarize our main findings, we discuss their significance and we draw our conclusions.

2 THE DEBRIS DISC

We consider a freely expanding Keplerian disc around the central object produced during the merger. This disc comprises the mass of the disrupted low-mass companion that has not been incorporated to the central object, as little mass is ejected from the system and carries the excess angular momentum of the progenitor binary system.

2.1 Evolution of the disc

As mentioned, for debris discs the outer boundary of the disc is free. That is, it is not tidally truncated like discs in binary systems but, instead, it may expand. Such discs are similar to discs formed by tidal disruption of stars by super-massive black holes (Cannizzo et al. 1990) or supernova fallback discs around young neutron stars, e.g. anomalous X-ray pulsars (Chatterjee et al. 2000; Alpar 2001). The model we employ is similar to the model proposed by Ertan et al. (2009) which describes the evolution of the thin disc in terms of its initial mass and angular momentum. This description of the evolution of the disc presumes that the cause of angular momentum transport in the disc is turbulent viscosity (Shakura & Sunyaev 1973) rather than hydromagnetic winds (Blandford & Payne 1982).

The temporal evolution of the surface mass density, Σ , in the disc is described by a diffusion equation (Pringle 1981):

$$\frac{\partial \Sigma}{\partial t} = \frac{3}{r} \frac{\partial}{\partial r} \left[r^{1/2} \frac{\partial}{\partial r} \left(\nu \Sigma r^{1/2} \right) \right] \quad (1)$$

where Σ is the surface mass density and ν is the turbulent kinematic viscosity. The rest of the thin disc structure equations (Frank et al. 2002) can be solved algebraically

(Cannizzo et al. 1990) to obtain a viscosity in the form $\nu = Cr^p \Sigma^q$ where C , p and q are constants determined by the opacity regime — see also Ertan et al. (2009). For this viscosity Eq. (1) is non-linear and has the self-similar solutions found by Pringle (1974). In the first type of solution (Cannizzo et al. 1990) the angular momentum of the disc is constant ($\dot{J}_d = 0$), but the mass of the disc evolves as a power-law in time. Specifically, the mass flow rate at the inner boundary can be expressed as:

$$\dot{M} = \dot{M}_0 \left(1 + \frac{t}{t_0} \right)^{-\alpha}, \quad \dot{M}_0 = (\alpha - 1) \frac{M_0}{t_0} \quad (2)$$

where t_0 is the viscous time-scale at some characteristic radius, M_0 the initial mass of the disc and \dot{M}_0 is the initial accretion rate. The power-law index α can be written in terms of p and q , which are determined by the opacity regime (Cannizzo et al. 1990). For electron scattering the exponent is $\alpha = 19/16$ and for the bound-free opacity regime is $\alpha = 5/4$. Hence, the difference between the two regimes is not large, and similar results can be found by changing the initial mass of the disc slightly. For our numerical simulations we use the bound-free regime as this would be the dominant opacity source for most of the lifetime of the system.

The second type of solutions describes a disc in which the mass of the disc is constant ($\dot{M}_d = 0$) while the angular momentum of the disc increases by the torque acted by the star (Pringle 1991). Such a disc would be relevant if the magnetosphere is rotating faster than the Keplerian velocity at the inner radius of the disc. This occurs in the so-called propeller regime (Illarionov & Sunyaev 1975) if the mass is retained in the disc rather than being ejected from the system.

The most important parameter governing the spin evolution of MWDs is the viscous time-scale t_0 , which is determined by the initial mass and angular momentum of the disc (Ertan et al. 2009). For our purposes, we assume a metal disc in the bound-free opacity regime with $\alpha_{SS} = 0.1$, where α_{SS} is the Shakura-Sunyaev viscosity, for which the viscous time-scale for the white dwarf debris disc is

$$t_0 \simeq 15 \text{ s} \left(\frac{j_0}{10^{18} \text{ cm}^2 \text{ s}^{-1}} \right)^{25/7} \left(\frac{M_0}{10^{-1} M_\odot} \right)^{-3/7} \quad (3)$$

where $j_0 = J_0/M_0$ is the total specific angular momentum. Note that the viscous time-scale depends strongly on j_0 and also on the opacity. However, if the source of opacity is electron scattering instead of bound-free transitions the viscous time-scale is changed at most by a factor of two. For a specific angular momentum one order of magnitude larger the viscous time-scale is of the order of 1 day, which is comparable to the 3 – 14 days estimate of Mochkovitch & Livio (1990).

2.2 Angular momentum evolution of the white dwarf

Angular momentum exchange between a disc and a star has been extensively studied since the discovery of X-ray pulsars, and these findings are nowadays applied to many astrophysical objects, like T Tauri stars and cataclysmic variables (Warner 1995). The strong magnetic field of the white

dwarf disrupts the inner part of the disc which would otherwise extend to the surface of the star. The inner radius of the disc, R_{in} , is determined by the balance between the magnetic and the material stresses. This is of the order of the Alfvén radius

$$R_A = \left(\frac{\mu_*^2}{\sqrt{2GM\dot{M}}} \right)^{2/7} \quad (4)$$

which, in the case of spherical accretion, is determined by the balance between magnetic and ram pressures (Davidson & Ostriker 1973). Here G is the gravitational constant, μ_* is the magnetic moment of the white dwarf and \dot{M} is the accretion rate reaching the inner radius but not necessarily accreting. Thus, we use $R_{\text{in}} = \xi R_A$ where ξ is a dimensionless factor used for converting the Alfvén radius for spherical accretion to the inner radius in disc accretion. In most studies — see e.g., Warner (1995) — $\xi \approx 0.5$ is usually adopted. Furthermore, numerical studies have shown that this value is applicable to the case of a dipolar field (Long et al. 2005). Nevertheless, when the accretion rate is so large that R_{in} is smaller than the radius of the star, we assume $R_{\text{in}} = R_{\text{WD}}$.

The way in which the star interacts with the disc depends on the interplay between its inner radius, the corotation radius, $R_{\text{co}} = (GM/\Omega_{\text{WD}}^2)^{1/3}$ where the disc is rotating with the same speed as the star, and the light cylinder radius, $R_L = c/\Omega_{\text{WD}}$, c being the speed of light. To model it, it is customary to define the fastness parameter (Ghosh & Lamb 1979; Lamb 1988, 1989) as

$$\omega_* = \frac{\Omega_{\text{WD}}}{\Omega_K(R_{\text{in}})} = \left(\frac{R_{\text{in}}}{R_{\text{co}}} \right)^{3/2}, \quad (5)$$

where $\Omega_K(R_{\text{in}})$ is the Keplerian angular velocity at the inner radius of the disc and Ω_{WD} is the angular velocity of the star. If the inner radius of the disc is smaller than the corotation radius ($\omega_* < 1$) the system is in the accretion regime. The inflowing matter at the inner edge of the disc will reach the surface of the star channelled by the magnetic field lines. If the inner disc radius is larger than the corotation radius ($\omega_* > 1$) accretion cannot occur due to the fast rotation of the star. This corresponds to the propeller regime (Illarionov & Sunyaev 1975; Wang & Robertson 1985). In this phase the disc continues its viscous evolution, though matter from the disc cannot be accreted on the star due to the centrifugal barrier.

The torque applied by the disc to the white dwarf is (Ghosh & Lamb 1979):

$$N_d = n(\omega_*)N_0. \quad (6)$$

where $N_0 = \Omega_K(R_{\text{in}})R_{\text{in}}^2\dot{M}$ and $n(\omega_*)$ is called the dimensionless torque. Following Alpar (2001) and Ekşi et al. (2005) we employ $n = 1 - \omega_*$. Consider a ring of mass Δm right outside the magnetospheric boundary $R_{\text{in}} + \Delta R$ where the flow is Keplerian. The angular momentum of the ring is $\Delta m(R_{\text{in}} + \Delta R)^2\Omega_K(R_{\text{in}} + \Delta R)$. Interaction with the magnetosphere will bring the matter to the angular velocity of the star at the magnetospheric boundary. The change in the angular momentum of the material is then $\Delta \ell = \Delta m(R_{\text{in}} + \Delta R)^2\Omega_K(R_{\text{in}} + \Delta R) - \Delta mR_{\text{in}}^2\Omega_*$. Assuming the transition region is narrow ($\Delta R \ll R_{\text{in}}$) and a continuous mass flow we obtain $N = \dot{M}R_{\text{in}}^2\Omega_K(R_{\text{in}})(1 - \omega_*)$. Hence

this prescription is equivalent to assuming that the magnetosphere and the accreting material are colliding “particles” and the interaction between them is inelastic.

If the inner radius of the disc goes beyond the light cylinder radius, the disc can no longer torque the star via the magnetosphere, $N_d = 0$. In this so-called ejector stage the star will spin-down via the magnetic dipole radiation torque

$$N_{\text{mdr}} = -\frac{2\mu_*^2 \sin^2 \beta \Omega_{\text{WD}}^3}{3c^3} \quad (7)$$

where β is the inclination angle between the magnetic and rotation axis.

We consider the effect of change in mass and radius of the star, which may be significant for those stars with masses close to the Chandrasekhar limit. In particular, the rotational velocity of the star depends on the moment of inertia of the star, which changes when a substantial amount of mass (of the order of about $0.1 M_{\odot}$) is accreted from the disc. In the case of accretion near the Chandrasekhar mass limit, the change in radius cannot be approximated by simple dependencies. Hence in our calculations we used the analytical mass-radius relationship of Nauenberg (1972)

$$R_* = 0.0126 R_{\odot} \left(\frac{R}{R_{\odot}} \right) \left(\frac{M}{M_{\odot}} \right)^{-1/3} \times \left[1 - \left(\frac{M}{M_{\text{Ch}}} \right)^{4/3} \right]^{1/2} \quad (8)$$

where

$$M_{\text{Ch}} = 1.435 M_{\odot} \left(\frac{2}{\mu} \right)^2 \quad (9)$$

An important effect of the change in radius is that due to flux conservation the strength of the magnetic field changes, $\Phi = B_{\text{WD}}R_{\text{WD}}^2$. This is also considered in our model. For the moment of inertia of white dwarfs we used

$$I_* = 3.2 \times 10^{50} \text{ g cm}^2 \left(\frac{M_*}{M_{\odot}} \right)^{0.34158} \times \left[1 - \left(\frac{M_*}{1.437 M_{\odot}} \right)^{1.25} \right]^{1.437} \quad (10)$$

which we obtained by fitting numerical results.

Finally, we introduce a critical temperature below which turbulence in the disc can not be sustained. We find the effective temperature using

$$T(r) = \left(\frac{3GM\dot{M}}{8\pi r^3 \sigma} \right)^{1/4} \left[1 - n \left(\frac{R_{\text{in}}}{r} \right)^{1/2} \right]^{1/4}. \quad (11)$$

(Frank et al. 2002) where $n \equiv N/\dot{M}\sqrt{GM R_{\text{in}}}$ is the dimensionless torque per unit mass accretion rate acted on the star.

3 RESULTS

3.1 Discs from SPH simulations

To compare our model with observations, we simulated the evolution of the merger remnants (namely, the white dwarf and the disc) using the results of the SPH simulations of

Table 1. Initial values of our simulations, as obtained from Lorén-Aguilar et al. (2009).

Run ($M_{\odot}+M_{\odot}$)	M_{WD} (M_{\odot})	M_0 (M_{\odot})	Ω_{WD} (s^{-1})	J_0 (g cm s^{-1})
0.5+0.3	0.62	0.18	0.134	1.40×10^{50}
0.8+0.4	0.92	0.28	0.244	2.65×10^{50}
0.8+0.6	1.10	0.30	0.401	2.85×10^{50}

Lorén-Aguilar et al. (2009). We restricted ourselves to those simulations for which the total mass of the system does not exceed M_{Ch} . The initial conditions used in our simulations — that is, the masses of the central remnant and the disc, the angular velocity of the uniformly rotating star and the angular momentum of the disc — are shown in Table 1.

For a given simulation, we calculated the spin evolution of the MWD for different polar field strengths. To determine the total integration time we used the simple cooling law of Mestel (1965) and the otherwise typical observed value of $T_{\text{eff}} \approx 40\,000$ K. The exact value of the initial core temperature depends on the mass of the merging components. However, its exact value has virtually no consequences in the age estimate, as white dwarfs cool very rapidly during the early phases of evolution. Consequently, we adopted an initial temperature of 10^8 K, a representative value of the SPH simulations. The cooling ages obtained in this way for the 0.5+0.3 M_{\odot} , 0.8+0.4 M_{\odot} and 0.8+0.6 M_{\odot} mergers — which result in MWDs of masses 0.8, 1.2, 1.4 M_{\odot} — were 13, 50 and 100 Myr respectively. It could be argued that for high core temperatures neutrino emission would shorten significantly the cooling times (Althaus et al. 2007). However, given the simplicity of the approach adopted here we consider that these cooling times are accurate enough. Moreover, we found that when these cooling times are compared with those obtained using full evolutionary calculations (Althaus et al. 2007; Salaris et al. 2010) the differences are minor.

In accordance with that explained in Sec. 2.2, the spin evolution of the star is determined by the fastness parameter, ω_* . Initially, the accretion rate is very large and the magnetospheric radius is small. In this case, the fastness parameter is smaller than 1. Thus, the inner radius of the disc is equal to the stellar radius and the rapid accretion of matter from the disc increases the angular momentum of the star. Hence, initially the remnants of mergers are fast rotators, and they spin at almost one third of the critical angular velocity of the star $\omega_* \approx 0.33$. This brief spin-up stage continues till $\omega_* > 1$. At this point the magnetic torque from the disc starts to spin down the star. At this stage the star can reach critical angular velocities if the mass of the white dwarf is close to M_{Ch} . This is due to the steep dependence of radius on mass near M_{Ch} . Since spin-down is only effective for $\omega_* > 1$, for very large accretion rates it might be possible that the star reaches critical rotation before the magnetospheric radius becomes larger than the stellar radius. This was the case for the simulations of Piersanti et al. (2003b), Piersanti et al. (2003a), Saio & Nomoto (2004), and Yoon et al. (2007). In our calculations this situation is avoided for the 0.5+0.3 M_{\odot} and the 0.8+0.4 M_{\odot} mergers. Hence, in the rest of the paper

we only discuss these calculations. Additionally, it could be possible that the star might spin-up to a point in which the inner radius exceeds the light cylinder and, thus, accretion ceases. In this case, magnetodipole spin-down (a less efficient mechanism) takes over. However, in our calculations we do not find this to be the case.

As the accretion rate decreases, the magnetospheric radius, hence ω_* , increases rapidly. This results in a stronger torque on the star which eventually forces it to reach equilibrium at $\omega_* \approx 1$. All our simulations evolve across this phase of torque transfer, and for all three cases there is a limiting magnetic field strength, B_{lim} , which determines whether a MWD will enter this strong spin-down phase, given the same cooling age. If the dipolar field strength, B_p , is close to B_{lim} the final period of the star is very sensitive to the exact value of B_p . In particular, near B_{lim} a 10% difference results in change by a factor of approximately 2 in the final spin period. Finally, after this strong spin down phase, if the magnetic field strengths and cooling age are adequate, the system reaches quasi-equilibrium around $\omega_* \lesssim 1$. This phase is called the tracking phase. The reason why a quasi-equilibrium phase is reached is that as mass transfer continues, the magnetospheric radius varies to match the corotation radius of the star. Hence, the star never reaches complete equilibrium and continues spinning down.

The aforementioned evolutionary phases are common for the 0.5+0.3 M_{\odot} and the 0.8+0.4 M_{\odot} simulations, and the final period of the object is determined by B_p , because in combination with the mass accretion rate, it determines the magnetospheric stopping radius, the fastness parameter, and thus the strength of the torque on the star for a given accretion rate. Since the accretion rate varies with time, the magnetic field strength of the star determines how fast the tracking phase is reached. In particular, if the dipolar field strength is large the tracking phase is reached earlier, because the associated torques are larger.

For the very early phases of evolution right after the merger, super-Eddington accretion rates are expected. This phase of the evolution is short (10^4 yr) with respect to the evolutionary time of the observed population of MWDs ($10^7 - 10^8$ yr), but it determines the maximum angular velocities attained at the beginning of disc evolution, due to the initial spin-up phase. However, for a given white dwarf and disc angular momentum, the spin at which the tracking phase is reached is determined by B_p . Actually, a simple relationship between B_p and the final period of the star can be easily computed. Taking into account that during the tracking phase the angular velocity of the star is almost equal to the Keplerian velocity at the inner radius of the disc, and the accretion is modelled by a power law, the period of the star can be written explicitly as:

$$\begin{aligned}
 P_* &= 3.4 \times 10^7 \text{ s} \left(\frac{M_*}{1.3 M_{\odot}} \right)^{-10/14} \left(\frac{B_p}{10^7 \text{ G}} \right)^{6/7} \\
 &\times \left(\frac{R_*}{4.3 \times 10^{-2} R_{\odot}} \right)^{18/7} \left(\frac{J_0}{2.5 \times 10^{50} \text{ g cm}^2 \text{ s}^{-1}} \right)^{25/28} \\
 &\times \left(\frac{t}{7.8 \times 10^7 \text{ yr}} \right)^{5/4}, \quad (12)
 \end{aligned}$$

which holds for $B_p > 10$ MG. The results of our calculations are shown in Fig. 1. As can be seen, although the periods obtained in this way are more or less consistent with the

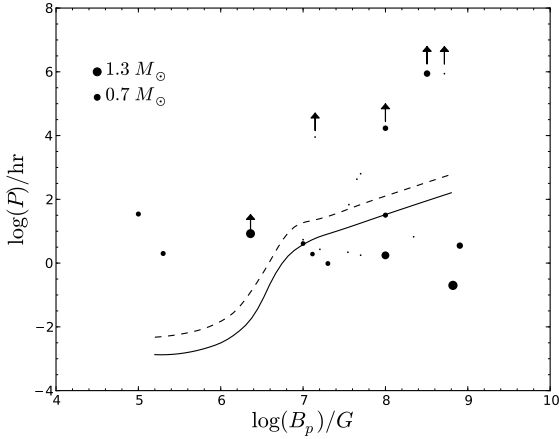


Figure 1. Period versus magnetic field strength for MWDs with known periods, compared to our results. The solid line corresponds to the case in which a $1.2 M_{\odot}$ MWD is considered, while the dashed line corresponds to the case of a $0.8 M_{\odot}$ star. The known MWDs (Kawka et al. 2007; Brinkworth et al. 2007) are represented using black circles. The mass of the object determines the size of the circle. The sizes of the circles for $1.3 M_{\odot}$ and $0.7 M_{\odot}$ stars are shown in the upper left corner of the figure. The stars with unknown masses are represented using small black dots. The data points with arrows indicate lower limits for the respective periods.

majority of periods of the population of MWDs, which have periods of days to weeks — see Kawka et al. (2007) and references therein — the majority of the observed spin periods seem to have a fairly flat distribution between 1 and 100 hr irrespective of the magnetic field. On the contrary, the models show a strong correlation with field strength in this range of periods. Before discussing this point we want to emphasize that not all magnetic white dwarfs have to be the result of a merger, and that our model is only aimed at reproducing the observed periods of massive white dwarfs. We elaborate on this point below.

3.2 Low-mass discs

Up to this point we have used an initial configuration directly derived from the results of the SPH simulations of Lorén-Aguilar et al. (2009). Consequently, we have assumed that during the initial phases of the evolution the central white dwarf accretes at the Eddington rate, in accordance with previous works — see Sect. 1. However, an alternative model recently proposed by Shen et al. (2012) assumes that the disc disperses its angular momentum due to shear in the differentially rotating layers. The reasoning of Shen et al. (2012) is based on the fact that radiative cooling is very inefficient. Hence, the material of the disc cannot relax to a thin disc configuration. This leads to entropy deposition within the disc due to viscous evolution. The detailed modelling of this phase was later done by Schwab et al. (2012) leading to viscous time scales of 10^4 s, within which the thick disc disperses and becomes thermally supported and spherically

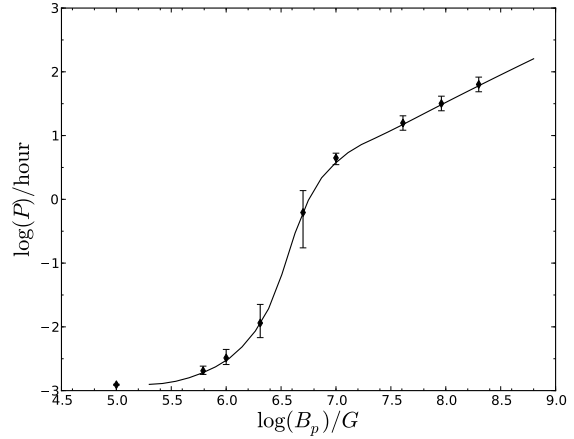


Figure 2. Comparison of the calculations in which the results of SPH simulations are adopted (solid line), and the simulations in which a low-mass disc was adopted (black dots), for a $1.2 M_{\odot}$ MWD. The error bars represent the results of the simulations with different disc angular momenta. The upper error bars are the periods obtained when the disc angular momentum is half of that resulting from the SPH simulations, whereas the lower periods result from simulations in which the angular momentum is a factor of two larger than that of the SPH calculations.

symmetric. Actually, Shen et al. (2012) find:

$$t_{\text{visc}} \approx \frac{1}{\alpha_{\text{SS}}} \left(\frac{r_{\text{cyl}}}{h} \right)^2 \left(\frac{r_{\text{cyl}}^3}{GM_0} \right)^{1/2} \approx 3 \times 10^4 \text{ s} \quad (13)$$

where h is the thickness of the disc, and r_{cyl} is its size.

This model, however, has two drawbacks. The first one is that the model assumes that no accretion occurs whatsoever. Consequently, the evolution of the disc is only governed by the change in angular momentum — see Sect. 2.1. This, in turn, forces the disc to evolve changing its angular momentum, as opposed to the case where the mass is allowed to be accreted on the central object, in which case the disc can expand to conserve its angular momentum. The second drawback of this model is the assumption that radiative energy losses within the disc are negligible. A very crude approximation using an electron scattering opacity and the initial surface density of the disc leads to

$$t_{\text{RL}} \approx \frac{h\kappa\Sigma_0}{c} \approx 2 \times 10^9 \text{ s} \quad (14)$$

where κ is the opacity of the disc. This time-scale is orders of magnitude longer than t_{visc} . However, both t_{visc} and t_{RL} depend strongly on r_{cyl} . As a matter of fact it turns out that $t_{\text{RL}}/t_{\text{visc}} \propto r_{\text{cyl}}^{-11/2}$. Hence, if the disc size increases during the evolution due to accretion on the central object, radiative cooling could become efficient and the disc would become thin. In our models, a thin disc reaches this size after 10^2 s if electron scattering is the dominant source of opacity. This is two orders of magnitude shorter than t_{visc} . It is, nevertheless, important to realize that up to now we have adopted a power law for \dot{M} . This approximation is safe for the later stages of the evolution, when most of the mass of the disc could be lost if the model of Shen et al. (2012) is valid. Hence, to estimate the final periods of the MWDs we also model these low-mass discs. In particular, we run a sec-

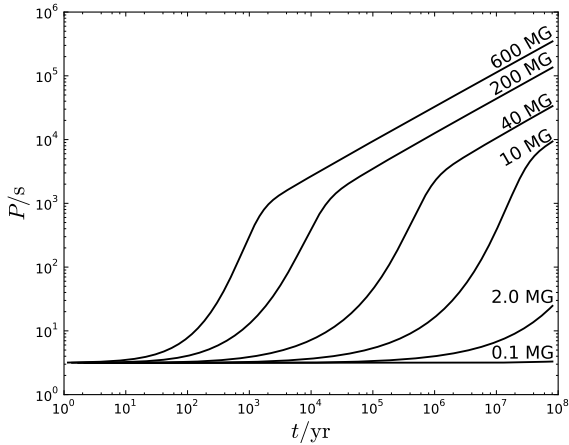


Figure 3. The evolution of the period of a $1.30 M_{\odot}$ MWD with a disc of mass $10^{-3} M_{\odot}$ for different initial magnetic field strengths.

ond set of simulations in which we adopted the same total mass of the system, but we assumed a disc mass $10^{-3} M_{\odot}$ — the mass of the disc when the Eddington accretion phase finishes and accretion driven by the evolution of angular momentum takes over — while the rest of the material was incorporated into the remnant white dwarf. We performed this test for the $0.8+0.4 M_{\odot}$ merger — which in this case results in a MWD of about $1.2 M_{\odot}$. Our results are shown in Fig. 2. As can be seen, the final periods of these simulations are almost identical to those previously presented. The reason for this is that the final periods reached at the end of the simulation for dipolar field strengths below B_{lim} are sensitive to the starting angular momentum of the star, since at this phase the star carries most of the angular momentum from the merger process. However, for stars with dipolar field strengths above B_{lim} , the final periods are determined by the angular momentum of the disc, see Eq. (12). This equation is valid for cooling ages longer than about 10^7 yr and $B_p > B_{\text{lim}} \approx 10$ MG, which apply for most high-field MWDs with known periods.

The angular momentum of the disc depends on the mass of the primary and the mass difference between the two components. As can be seen in Table 1, the angular momenta of the mergers studied by Lorén-Aguilar et al. (2009) differ by about a factor of two. To simulate arbitrary mass ratios, we made trial runs with different disc angular momenta within a factor of 2 of those obtained in the SPH simulations — see Fig. 2. Our calculations show that, except for the case in which the magnetic field strengths are close to B_{lim} — that is, when the evolution is stopped just before the quasi-equilibrium phase is reached — the results are nearly identical to those in which the angular momentum resulting from the SPH simulations is adopted. In fact, although for the strong torque transfer phase the periods can differ by an order of magnitude, for the tracking phase the maximum difference in the computed periods is approximately 20%.

3.3 Some insight from RE J 0317–853 and WD 1658+441

To compare our results with the properties of two known ultra-massive MWDs which are supposed to be the result of a merger — namely RE J 0317–853 and WD 1658+441 — we followed the evolution of a remnant with their approximate mass, $1.30 M_{\odot}$. For this simulation we adopted the following initial conditions. The initial angular momentum was $J_0 = 2.5 \times 10^{50}$ g cm s $^{-1}$, whereas the initial angular velocity was $\Omega_K/3$. We remind the reader that, according to that discussed in Sect. 3.2, the value of the initial angular momentum plays a limited role, whilst the initial value of the angular velocity does not have a large impact in our results as long as we only consider the values of the periods obtained during the tracking phase. The observed period of RE J 0317–853 is 721 s (Barstow et al. 1995; Ferrario et al. 1997), whilst in the case of WD 1658+441 no conclusive evidence of rotation has been found so far (Schmidt et al. 1992). However, for this last object the instrumental timing limit of 8.4 h can be adopted as a lower limit to the period (Shtol’ et al. 1997). The magnetic field strength of RE J 0317–853 is between 170 MG and 660 MG (Ferrario et al. 1997; Burleigh et al. 1999; Vennes et al. 2003; Ferrario & Wickramasinghe 2005), the magnetic field strength of WD 1658+441 is estimated to be 2.3 MG (Schmidt et al. 1992). For these specific simulations we stopped the simulations at the cooling age for which $T_{\text{eff}} \approx 40\,000$ K, a value consistent with the observational determination for RE J 0317–853 (Barstow et al. 1995; Ferrario et al. 1997; Vennes et al. 2003) and 30 000 K, the effective temperature of WD 1658+441. However, we stress that if $T_{\text{eff}} = 40\,000$ K is taken as an upper limit, the final ages for both objects are lower limits ($t_{\text{cool}} \approx 10^8$ yr) and consequently the computed periods are also lower limits. The evolution of the period as a function of time is shown in Fig. 3. Clearly, Fig. 3 reveals that our simulations cannot reproduce the observed properties of these objects, and that another braking mechanism must operate. In particular, for RE J 0317–853 our model predicts a period which is much longer than that observationally determined, while for WD 1658+441, which has a smaller magnetic field, we obtain periods of the order of 10^2 s, much shorter than expected. More generally, for dipole magnetic field strengths larger than $B_{\text{lim}} \approx 10$ MG — namely, for the case of RE J 0317–853 — the periods are longer than about 10^4 s, while for field strengths smaller than this value — which is the case of WD 1658+441 — the spin-down mechanisms implemented in our model are not adequate either. Hence, our simulations show that neither viscous dissipation nor magneto-dipole spin-down are able to explain the observed periods of these objects, confirming our previous finding that other alternatives must be sought.

3.4 Models with turbulence turn-off

An important question to be analysed is whether turbulence in the accretion disc can be sustained efficiently during the entire lifetime of MWDs. This question is relevant when the lifetimes of neutron stars with fallback discs and MWDs are compared. In the former case the evolutionary ages are typically $10^4 - 10^5$ yr, whilst the lifetimes of MWDs are three

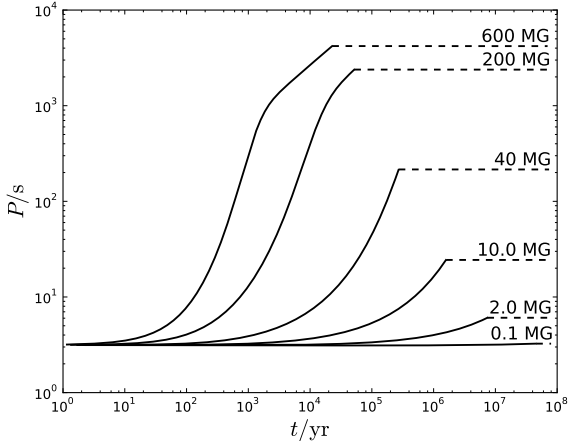


Figure 4. The evolution of the period for a $1.30 M_{\odot}$ MWD. The simulations are identical to those of Fig. 3, except for the inclusion of turbulence turn-off at $T_p = 1000$ K. The dashed lines correspond to the phase during which the torque transfer from the disc becomes ineffective and magneto-dipole spin down takes over.

to four orders of magnitude longer. Thus, this question is an important factor to be considered.

Whether the disc is turbulent or not is mainly determined by the degree of ionisation of the disc material. That is, the existence of turbulence depends on the temperature, which, in turn, is determined by the accretion rate — see Eq. (11). The ionisation stability of accretion discs has been investigated thoroughly by Menou et al. (2001). In their work they computed the thermal equilibrium (the so-called S-curves) of thin accretion discs with different chemical compositions, and showed that for thin discs made of C, thermal equilibrium is reached near 5000 K, and that for all compositions recombination always occurs below approximately 1000 K. For the conditions found during the final stages of our simulations these temperatures are relatively high. However, it is known that these discs can be partially ionised at even lower temperatures, due to several other processes, like cosmic ray heating, collisions and charged-particle mobility. Inutsuka & Sano (2005) carefully studied all these effects and reached the conclusion that at temperatures below about 1000 K, magneto-rotational instability (MRI) could be still effective. Building upon their work, Ertan et al. (2009) modelled the evolution of debris discs assuming that the differentially-rotating layers with temperatures smaller than a critical temperature, T_p , do not change the angular momentum of the star. Moreover, they showed that when $T_p \approx 100$ K is adopted the observations are consistently reproduced.

Contrary to the modelling of Ertan et al. (2009), in which turbulence is switched-off layer by layer, we applied a simpler procedure to test for how long the disk would be turbulent. For each time step, we calculated the temperature at $r = 10R_{\text{in}}$. If this temperature was smaller than $T_p = 1000$ K, we assumed that the disc was not turbulent and accretion was switched-off. Thus, the MWD immediately enters in the so-called ejector phase and spins down only due to magneto-dipole radiation. To compare these calculations to the case of RE J 0317–853 and WD 1658+441

we applied this procedure to the model of $1.3 M_{\odot}$ described in Sec. 3.2. We found that although the MRI is long-lived (about $10^5 - 10^7$ yr), the disc becomes inactive at the current ages of these objects (about 10^8 yr). Moreover, since the magneto-dipole torque is not as strong as the magnetic torque from the disc, the final period is determined by the time at which MRI is turned off, which depends on the accretion rate, and can be determined from Eq. (11):

$$\begin{aligned}
 P_* &= 1.3 \times 10^3 \text{ s} \left(\frac{M_*}{1.3 M_{\odot}} \right)^{-10/28} \\
 &\times \left(\frac{\dot{M}_*}{2.2 \times 10^{-11} M_{\odot} \text{ yr}^{-1}} \right)^{1/28} \\
 &\times \left(\frac{B_p}{10^8 \text{ MG}} \right)^{3/7} \left(\frac{R_*}{4.3 \times 10^{-3} R_{\odot}} \right)^{-9/7} \\
 &\times \left(\frac{T_p}{1000 \text{ K}} \right). \quad (15)
 \end{aligned}$$

As can be seen in Fig. 4, the accretion rate at the time of MRI deactivation depends also in the strength of the magnetic field. If the torque exerted by the disc is strong enough, the disc becomes inactive after reaching the tracking phase. For $T_p = 1000$ K, for white dwarfs of masses between 0.8 and $1.3 M_{\odot}$ this occurs for magnetic fields around 90 MG. In this case, the final period of the star is determined by B_p and the critical temperature of MRI turn-off. Using Eq. (11) once more, the value of \dot{M} at the point at which T_p is reached can be determined, and employing this value, the period at the time of MRI turn-off can be computed:

$$\begin{aligned}
 P_* &= 1.3 \times 10^3 \text{ s} \left(\frac{M_*}{1.3 M_{\odot}} \right)^{-5/13} \\
 &\times \left(\frac{R_*}{4.3 \times 10^{-3} R_{\odot}} \right)^{18/13} \\
 &\times \left(\frac{B_p}{10^8 \text{ G}} \right)^{6/13} \left(\frac{T_p}{1000 \text{ K}} \right)^{-12/13}. \quad (16)
 \end{aligned}$$

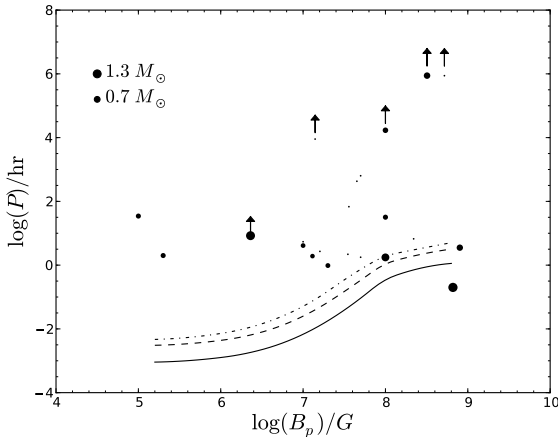
This expression shows that for MWDs with field strengths between 50 MG and 1 GG, and T_p ranging from 300 K to 1000 K, the final periods reached are around $10^3 - 10^4$ s (see also Fig. 4).

In Fig. 5 we compare the results of these calculations with the observational data. This is done for three white dwarfs masses, $0.8 M_{\odot}$, $1.0 M_{\odot}$ and $1.3 M_{\odot}$. As can be seen in this figure, now the computed periods are considerably shorter, and match better the periods of MWDs with known masses. However, in order to perform a meaningful comparison with the observations only those MWDs which are likely to be the result of a merger need to be considered. Thus, we removed all MWDs with masses smaller than $0.8 M_{\odot}$. Of these MWDs six have known periods. Three of them are well known slow rotators, namely Grw +70°8247, G 240–72 and WD 1658+441, for which only lower limits to their periods have been determined. The remaining three are PG 1015+014, PG 1031+234 and RE J 0317–853, which all have magnetic fields above 50 MG, and periods of the order of an hour or less. We simulated the secular evolution of the spin of these three MWDs, using the observationally determined values of their masses and magnetic field strengths —

Table 2. Comparison of the simulated and observational data, when a an MRI turn-off temperature $T_p = 1000$ K is adopted.

WD	Other names	M_{WD} (M_{\odot})	B (MG)	B_p (MG)	P_{obs} (min)	P_{sim} (min)	Refs.
0325–857	RE J 0317–853	1.35	170–660	200	12.08	28	1,2,3
1015+014	PG 1015+014	1.15	50–90	90	$98.84^{+0.14}_{-0.07}$	36	4,5,6
1031+234	PG 1031+234	0.93	200–1000	500	211.8 ± 3.0	205	4,6,7

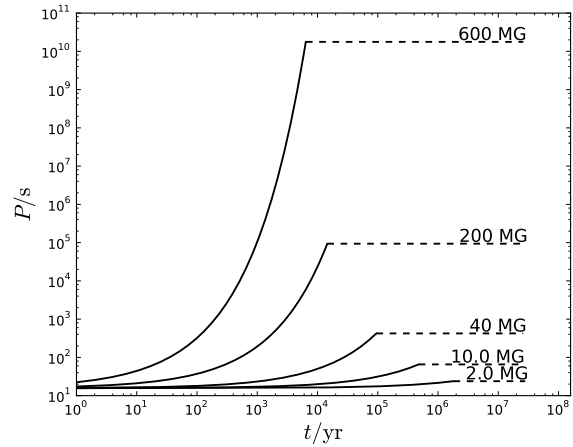
- (1) Barstow et al. (1995), (2) Ferrario et al. (1997), (3) Külebi et al. (2010), (4) Liebert et al. (2003),
(5) Euchner et al. (2006), (6) Brinkworth et al. (2007), (7) Schmidt et al. (1986)


Figure 5. Same as Fig. 1 for the simulations in which turbulence is switched-off at $T_p = 1000$ K. The solid line represents the spin evolution of a MWD of $1.3 M_{\odot}$, the dashed line that of a MWD of mass $1.0 M_{\odot}$, and dot-dashed one corresponds to the case in a mass of $0.8 M_{\odot}$ is adopted.

see Table 2. In addition to the properties of the disc, the most important input in our simulations is the dipolar magnetic field strength. Specifically, it has been shown that probably RE J 0317–853 (Barstow et al. 1995; Ferrario et al. 1997; Vennes et al. 2003), PG 1031+234 (Schmidt et al. 1986) and PG 1015+014 (Euchner et al. 2006) have dipolar field components considerably smaller than the maximum observed field strength. Thus, for them we adopt the values listed in the fifth column of Table 2, which in general are somewhat smaller than the observed surface field strengths. The results of our simulations are shown in Table 2. We note that the simulated periods for these three MWDs (listed in the seventh column of this table) compare favourably with the observed periods (sixth column). In particular, for RE J 0317–853 the computed period is a factor of two longer, while for PG 1015+014 is a factor of three shorter, and for PG 1031+234 we find a nice agreement. All this indicates that these objects were most likely originated in a merger, and subsequently lost their angular momentum due to the magnetospheric interaction with a remnant disc.

3.5 Winds

It is currently understood that the initial rapid accretion phase can not be approximated by cold accretion, and that a hot region around the central MWD would be formed — see, e.g., van Kerkwijk et al. (2010). In order to qualitatively


Figure 6. The evolution of the period of a $1.1 M_{\odot}$ MWD due to torques from the wind with turbulence turn-off at $T_p = 1000$ K. The initial conditions were those obtained in the SPH simulation of the merger of two $0.8+0.6 M_{\odot}$ white dwarfs (see Table 1).

understand the implications of this for the angular momentum evolution of a MWD, we built a model in which the spin down is due to the outflow of the material rather than to accretion onto the star. In this prescription, mass transfer between the disc and the star occurs, but the material is not bound to the system, and it is ejected.

The induced torques on the star can be then approximated by wind torques (Weber & Davis 1967):

$$N_w = -\eta \dot{M}_w \Omega_* R_A^2 \quad (17)$$

where \dot{M}_w is the wind mass loss rate, and η is a parameter which depends on the geometry of the mass loss, which for a spherically symmetric wind is $2/3$. In this expression the Alfvén radius R_A is computed as the distance at which the Alfvén speed equals the wind velocity, rather than the incoming velocity of the accreting material, as in Eq. (4). Note that R_A depends on the geometry of the magnetic field, and simulations are necessary for precise values — see, for instance, Matt & Pudritz (2005, 2008). However, for the sake of simplicity, we assume that the mass-loss rate follows the same power law given by Eq. (2) and that R_A is that corresponding to disc accretion.

We find that during the early phases of the evolution the spin rates are not strongly affected, since the mass-loss rates are very high, and R_A is small. However, as the mass-loss rate decreases R_A becomes larger, and a strong torque on the object is exerted. In fact, the most apparent qualitative difference between the wind and the disc spin down scenarios

is that in the first one the torque spins down the MWD most effectively at relatively early phases of its evolution, before reaching a quasi-equilibrium, whereas in the second one the wind spin down is ineffective during the initial phases of the evolution, and as the mass-loss rate drops, the torque rapidly becomes stronger. Moreover, in this case the period evolution can be calculated analytically, once it is taken into account that the only time-dependent quantity now is \dot{M} :

$$\ln\left(\frac{P}{P_0}\right) \propto \frac{\kappa}{I_*} M_*^{2/7} R_*^{24/7} M_0^{3/7} t_0^{3/28} B^{8/7} t^{13/28} \quad (18)$$

where P_0 is the initial period of the star. This expression indicates that the final periods of MWDs are very sensitive to the values of the stellar parameters, and that depending on their precise value large spin downs might be obtained.

We are interested in estimating the time needed to reach periods similar to that of RE J 0317–853, i.e. $P_* \approx 10^4$ s. Assuming that the initial period is about 10 s, the corresponding time-scale is:

$$\begin{aligned} t_{\text{MWD}} &\approx 2.35 \times 10^5 \text{ yr} \left(\frac{2/3}{\eta} \frac{I_*}{5.4 \times 10^{49} \text{ g cm}^2} \right)^{28/13} \\ &\times \left(\frac{M_*}{1.1 M_\odot} \right)^{-8/13} \left(\frac{R_*}{7 \times 10^{-3} R_\odot} \right)^{-56/13} \\ &\times \left(\frac{M_0}{0.3 M_\odot} \right)^{-12/13} \left(\frac{t_0}{1 \text{ s}} \right)^{-3/13} \left(\frac{B}{10^8 \text{ G}} \right)^{-32/13} \quad (19) \end{aligned}$$

For strong dipolar field strengths periods of the order of 10^3 seconds are reached in time-scales much smaller than the cooling age of RE J 0317–853 and similar objects. Additionally, our simulations with turbulence turn-off show that for MWDs with field strengths larger than 200 MG the wind spin down is effective long enough to induce strong spin down — see Fig. 6. We also note that in this case the resulting periods are similar to those of Grw +70°8247 and GD 229, which > 100 yr — see Kawka et al. (2007) and references therein. On the contrary, for field strengths smaller than about 50 MG, the wind torques are ineffective, yielding periods smaller than a few minutes ($P_* < 3 \times 10^2$ s) which are unrealistic for the observed periods of the MWDs.

4 CONCLUSIONS

We have studied the long-term evolution of magnetic white dwarfs surrounded by debris discs, which are thought to be the final products of the merger of two degenerate cores. To do so we built a simple model to follow the coupling between the central object and the surrounding disc. This model is similar to those used to study supernova fallback discs around young neutron stars, and presumes that the evolution of the disc is dominated by angular momentum transport by turbulent viscosity. Contrary to previous studies of the evolution of discs around white dwarfs, our model considers a freely expanding Keplerian disc. Using this model we found that for these systems there is a relation between the mass, the rotation period, and the strength of the magnetic field.

In a first set of simulations we studied the evolution of the merger remnants using the results of detailed SPH simulations and assuming that the entire disc was turbulent.

For these models we found that the final spin of the white dwarf is given by a simple relation — see Eq. (12). However, the periods obtained in this way are somewhat larger than the observed ones. Consequently, we studied other alternatives. In particular, in a second set of simulations we computed a set models in which we assumed — in accordance with the studies of Yoon et al. (2007); van Kerkwijk et al. (2010); Shen et al. (2012) — that the cold accretion assumption would not be applicable to the post merger systems. Following the suggestion of Nordhaus et al. (2011), we simulated the case in which the mass transferred from the discs would end up as an outflow, and the spin down is governed by the magnetic interaction with it. We found that, nevertheless, the periods obtained in this second set of models are again too large. We also varied by a factor of two the initial angular momentum of the disc, and we also found that the resulting periods do not differ much from those obtained using the results of the SPH simulations. All this led us to analyse whether turbulence in the accretion disc can be sustained efficiently during the entire lifetime of MWDs. This depends mainly on the degree of ionisation of the disc material. According to the most recent studies we assumed that turbulence ceases when the temperature of the disc is smaller than a certain threshold, for which we adopted $T_p = 1000$ K (Inutsuka & Sano 2005). When this model is adopted our calculations reproduce the observed properties of three MWDs with known masses and periods in the solar neighbourhood which are massive enough — namely, with masses larger than $0.8 M_\odot$ — to be considered the result of white dwarf binary mergers (RE J 0317–853, PG 1015+014, and PG 1031+234). These findings support the hypothesis that these white dwarfs are the remnants of double-degenerate mergers that have gone through magnetospheric interaction with a remnant disc. More specifically, it has been known for a long time that RE J 0317–853, the fastest rotator within the MWD population, spins slower than what it should be expected for a double white dwarf merger. Our model reproduces the rotation period of this object, which was previously unaccounted for. However, we also find that our model cannot explain the properties of the rest of the population of massive MWDs, which is probably formed by multiple evolutionary channels Ferrario & Wickramasinghe (2005). In particular, there are three massive MWDs (Grw +70°8247, G 240–72 and WD 1658+441) which are slow rotators, and probably have experienced spin-down during the red giant phase either as a single star or after a core merger during the common envelope phase, as suggested by Tout et al. (2008).

Ferrario & Wickramasinghe (2005) conducted very thorough observational investigations of the properties of the population of MWDs and resolved that within it there are three different magnetic field and period intervals, which point out towards different evolutionary origins. Specifically, they proposed the existence of three distinct groups of stars. The first group corresponds to a population of magnetized slow rotators — with typical periods ranging from $P \approx 50$ yr to 100 yr — which most likely have evolved from isolated progenitors. To the best of our knowledge only one qualitative study of the evolution of rotating MWDs originating from single stars has been performed so far. Specifically, Suijs et al. (2008) estimated the effect of magnetism on the core rotation and concluded that the presence of magnetic

fields leads to slower rotating cores. However, their results do not fully account for the long rotation periods of some MWDs, namely those belonging to the tail of the distribution (with periods longer than about 100 yr). For these stars they proposed that spin-down by stellar winds might be an effective alternative. However, a binary origin for this group of stars cannot be discarded, as the results of Tout et al. (2008) show that a merger during the common envelope phase can result as well in a slowly rotating MWD. A second group of stars is that of strongly magnetized fast rotators ($P \approx 700$ s), which probably carry the remnant angular momentum from the double-degenerate merger. Finally, there exists a third group of rotators with periods ranging from hours to days, which may have a mixed origin. Additionally, they found that the majority of MWDs have periods between a few hours to a few weeks, and also that the known slow rotators are not all necessarily highly magnetic (e.g. WD 1658+441). However, although the overall picture drawn by Ferrario & Wickramasinghe (2005) may not be significantly altered by our calculations, our results indicate that the distinction between all three groups may not be so clear — see Fig. 5. Moreover, our results show that slow rotation does not provide sufficient evidence to discard a binary evolutionary origin of individual MWDs, since also the dipole field strength, the mass and the age of the specific star need to be considered.

Additionally, our scenario predicts the existence of a population of MWDs surrounded by dust discs. Observational searches of dust discs around two massive MWDs (REJ 0317–853 and WD 1658+441) have been performed using the *Spitzer* telescope, but no discs have been detected so far (Hansen et al. 2006). However, the lack of detection of debris discs around high-field MWDs (those with $B > 2$ MG) might be due to the diffuse structure resulting from their large magnetospheric stopping radii — a consequence of the large magnetic pressure of the remnant of the merger — which, in turn, produces an extended disc. More generally, our models imply that the detectability of a remnant disc depends not only on the mass of the MWD, but also on its magnetic field strength and on its period. Clearly, deeper observations are needed to confirm the existence of these diffuse discs around MWDs. In this regard it is important to mention the recent discovery of an unveiled population of MWDs surrounded by dust discs. NLTT 10480 (Kawka & Vennes 2011) and G77–5018 (Farihi et al. 2011) are examples of MWDs with significant infrared excesses, which could be attributed to the existence of debris disc around them.

Finally, we would like to mention that one important hindrance of our modelling is the difference between the geometry of the magnetic field assumed in our simulations and that of the observed MWD population. Multi-phase spectropolarimetric analysis (Euchner et al. 2002, 2005) and single phase spectral studies (Külebi et al. 2009) of a large number of MWDs have showed that their field geometry is more complicated than a simple dipole, as it is assumed in our simplified model. This is an important issue as numerical simulations show that the geometry of the magnetic field is important for determining the magnetospheric stopping radius of an accreting star (Long et al. 2007, 2008, 2012). For the case of REJ 0317–853 and PG 1031+234 — two of the specific white dwarfs analysed here — we addressed

this issue by assuming dipolar field strengths smaller than the total measured value of the magnetic field, a simple but effective procedure. Thus, future studies in this direction should adopt more realistic magnetic configurations.

ACKNOWLEDGMENTS

This work was partially supported by MCINN grant AYA2011–23102, by the European Union FEDER funds, and by the ESF EUROGENESIS project (grant EUI2009-04167). We would like to thank Aldo Serenelli for many fruitful discussions during the course of this research.

REFERENCES

- Alpar M. A., 2001, *ApJ*, 554, 1245
 Althaus L. G., García-Berro E., Isern J., Córscico A. H., Rohrmann R. D., 2007, *A&A*, 465, 249
 Angel J. R. P., Borra E. F., Landstreet J. D., 1981, *ApJS*, 45, 457
 Barstow M. A., Jordan S., O’Donoghue D., Burleigh M. R., Napiwotzki R., Harrop-Allin M. K., 1995, *MNRAS*, 277, 971
 Blandford R. D., Payne D. G., 1982, *MNRAS*, 199, 883
 Bloom J. S., Kasen D., Shen K. J., Nugent P. E., Butler N. R., Graham M. L., Howell D. A., Kolb U., Holmes S., Haswell C. A., Burwitz V., Rodriguez J., Sullivan M., 2012, *ApJL*, 744, L17
 Brinkworth C. S., Burleigh M. R., Marsh T. R., 2007, in R. Napiwotzki & M. R. Burleigh ed., 15th European Workshop on White Dwarfs Vol. 372 of *Astronomical Society of the Pacific Conference Series*, A Survey for Photometric Variability in Isolated Magnetic White Dwarfs – Measuring their Spin Periods. p. 183
 Brinkworth C. S., Gänsicke B. T., Marsh T. R., Hoard D. W., Tappert C., 2009, *ApJ*, 696, 1402
 Burleigh M. R., Jordan S., Schweizer W., 1999, *ApJL*, 510, L37
 Cannizzo J. K., Lee H. M., Goodman J., 1990, *ApJ*, 351, 38
 Chatterjee P., Hernquist L., Narayan R., 2000, *ApJ*, 534, 373
 Dan M., Rosswog S., Guillochon J., Ramirez-Ruiz E., 2012, *MNRAS*, 422, 2417
 Davidson K., Ostriker J. P., 1973, *ApJ*, 179, 585
 Dobbie P. D., Baxter R., Kulebi B., Parker Q. A., Koester D., Jordan S., Lodieu N., Euchner F., 2011, *ArXiv e-prints*
 Dufour P., Bergeron P., Schmidt G. D., Liebert J., Harris H. C., Knapp G. R., Anderson S. F., Schneider D. P., 2006, *ApJ*, 651, 1112
 Ekşi K. Y., Hernquist L., Narayan R., 2005, *ApJL*, 623, L41
 Ertan Ü., Ekşi K. Y., Erkut M. H., Alpar M. A., 2009, *ApJ*, 702, 1309
 Euchner F., Jordan S., Beuermann K., Gänsicke B. T., Hesterman F. V., 2002, *A&A*, 390, 633
 Euchner F., Jordan S., Beuermann K., Reinsch K., Gänsicke B. T., 2006, *A&A*, 451, 671
 Euchner F., Reinsch K., Jordan S., Beuermann K., Gänsicke B. T., 2005, *A&A*, 442, 651

- Farihi J., Dufour P., Napiwotzki R., Koester D., 2011, *MNRAS*, 413, 2559
- Ferrario L., Vennes S., Wickramasinghe D. T., Bailey J. A., Christian D. J., 1997, *MNRAS*, 292, 205
- Ferrario L., Wickramasinghe D. T., 2005, *MNRAS*, 356, 615
- Frank J., King A., Raine D. J., 2002, *Accretion Power in Astrophysics: Third Edition*. Cambridge University Press
- Gänsicke B. T., Koester D., Marsh T. R., Rebassa-Mansergas A., Southworth J., 2008, *MNRAS*, 391, L103
- Gänsicke B. T., Marsh T. R., Southworth J., 2007, *MNRAS*, 380, L35
- García-Berro E., Lorén-Aguilar P., Aznar-Siguán G., Torres S., Camacho J., Althaus L. G., Córscico A. H., Külebi B., Isern J., 2012, *ApJ*, 749, 25
- García-Berro E., Lorén-Aguilar P., Pedemonte A. G., Isern J., Bergeron P., Dufour P., Brassard P., 2007, *ApJL*, 661, L179
- Ghosh P., Lamb F. K., 1979, *ApJ*, 234, 296
- Guerrero J., García-Berro E., Isern J., 2004, *A&A*, 413, 257
- Hansen B. M. S., Kulkarni S., Wiktorowicz S., 2006, *AJ*, 131, 1106
- Iben Jr. I., Tutukov A. V., 1984, *ApJS*, 54, 335
- Illarionov A. F., Sunyaev R. A., 1975, *A&A*, 39, 185
- Inutsuka S.-i., Sano T., 2005, *ApJL*, 628, L155
- Jordan S., Aznar Cuadrado R., Napiwotzki R., Schmid H. M., Solanki S. K., 2007, *A&A*, 462, 1097
- Kawka A., Vennes S., 2011, *A&A*, 532, A7
- Kawka A., Vennes S., Schmidt G. D., Wickramasinghe D. T., Koch R., 2007, *ApJ*, 654, 499
- Kepler S. O., Kleinman S. J., Nitta A., Koester D., Castanheira B. G., Giovannini O., Costa A. F. M., Althaus L., 2007, *MNRAS*, 375, 1315
- Kilic M., Redfield S., 2007, *ApJ*, 660, 641
- King A. R., Pringle J. E., Wickramasinghe D. T., 2001, *MNRAS*, 320, L45
- Külebi B., Jordan S., Euchner F., Gänsicke B. T., Hirsch H., 2009, *A&A*, 506, 1341
- Külebi B., Jordan S., Nelan E., Bastian U., Altmann M., 2010, *A&A*, *in press*, arXiv:1007.4978
- Lamb D. Q., 1988, *Theory of magnetic cataclysmic binary X-ray sources*. Vatican Obs., pp 151–197
- Lamb F. K., 1989, in H. Ögelman & E. P. J. van den Heuvel ed., *Timing Neutron Stars Accretion by magnetic neutron stars*. p. 649
- Levan A. J., Wynn G. A., Chapman R., Davies M. B., King A. R., Priddey R. S., Tanvir N. R., 2006, *MNRAS*, 368, L1
- Liebert J., Bergeron P., Holberg J. B., 2003, *AJ*, 125, 348
- Liebert J., Wickramasinghe D. T., Schmidt G. D., Silvestri N. M., Hawley S. L., Szkody P., Ferrario L., Webbink R. F., Oswalt T. D., Smith J. A., Lemagie M. P., 2005, *AJ*, 129, 2376
- Long M., Romanova M. M., Lamb F. K., 2012, *New Astron.*, 17, 232
- Long M., Romanova M. M., Lovelace R. V. E., 2005, *ApJ*, 634, 1214
- Long M., Romanova M. M., Lovelace R. V. E., 2007, *MNRAS*, 374, 436
- Long M., Romanova M. M., Lovelace R. V. E., 2008, *MNRAS*, 386, 1274
- Lorén-Aguilar P., Isern J., García-Berro E., 2009, *A&A*, 500, 1193
- Marsh M. C., Barstow M. A., Buckley D. A., Burleigh M. R., Holberg J. B., Koester D., O’Donoghue D., Penny A. J., Sansom A. E., 1997, *MNRAS*, 287, 705
- Matt S., Pudritz R. E., 2005, *ApJL*, 632, L135
- Matt S., Pudritz R. E., 2008, *ApJ*, 678, 1109
- Menou K., Perna R., Hernquist L., 2001, *ApJ*, 559, 1032
- Mestel L., 1965, *Stars in Stellar Systems*. University of Chicago Press, Chicago, 1965
- Mochkovitch R., Livio M., 1990, *A&A*, 236, 378
- Nauenberg M., 1972, *ApJ*, 175, 417
- Nomoto K., Iben Jr. I., 1985, *ApJ*, 297, 531
- Nordhaus J., Wellons S., Spiegel D. S., Metzger B. D., Blackman E. G., 2011, *Proceedings of the National Academy of Science*, 108, 3135
- Paczynski B., 1991, *ApJ*, 370, 597
- Piersanti L., Gagliardi S., Iben Jr. I., Tornambé A., 2003a, *ApJ*, 598, 1229
- Piersanti L., Gagliardi S., Iben Jr. I., Tornambé A., 2003b, *ApJ*, 583, 885
- Piro A. L., 2008, *ApJ*, 679, 616
- Piro A. L., Bildsten L., 2007, *ApJ*, 663, 1252
- Popham R., Narayan R., 1991, *ApJ*, 370, 604
- Potter A. T., Tout C. A., 2010, *MNRAS*, 402, 1072
- Pringle J. E., 1974, *PhD thesis*, Univ. Cambridge, (1974)
- Pringle J. E., 1981, *ARAA*, 19, 137
- Pringle J. E., 1991, *MNRAS*, 248, 754
- Reid I. N., Liebert J., Schmidt G. D., 2001, *ApJL*, 550, L61
- Saio H., Nomoto K., 2004, *ApJ*, 615, 444
- Salaris M., Cassisi S., Pietrinferni A., Kowalski P. M., Isern J., 2010, *ApJ*, 716, 1241
- Schaefer B. E., Pagnotta A., 2012, *Nature*, 481, 164
- Schmidt G. D., Bergeron P., Liebert J., Saffer R. A., 1992, *ApJ*, 394, 603
- Schmidt G. D., West S. C., Liebert J., Green R. F., Stockman H. S., 1986, *ApJ*, 309, 218
- Schwab J., Shen K. J., Quataert E., Dan M., Rosswog S., 2012, *ArXiv e-prints*
- Shakura N. I., Sunyaev R. A., 1973, *A&A*, 24, 337
- Shen K. J., Bildsten L., Kasen D., Quataert E., 2012, *ApJ*, 748, 35
- Shtol’ V. G., Valyavin G. G., Fabrika S. N., Bychkov V. D., Stolyarov V. A., 1997, *Astronomy Letters*, 23, 48
- Suijs M. P. L., Langer N., Poelarends A.-J., Yoon S.-C., Heger A., Herwig F., 2008, *A&A*, 481, L87
- Tout C. A., Wickramasinghe D. T., Liebert J., Ferrario L., Pringle J. E., 2008, *MNRAS*, 387, 897
- Tutukov A. V., Yungelson L. R., 1979, *Acta Astron.*, 29, 665
- van Kerkwijk M. H., Chang P., Justham S., 2010, *ApJL*, 722, L157
- Vennes S., Kawka A., 2008, *MNRAS*, 389, 1367
- Vennes S., Schmidt G. D., Ferrario L., Christian D. J., Wickramasinghe D. T., Kawka A., 2003, *ApJ*, 593, 1040
- von Hippel T., Kuchner M. J., Kilic M., Mullally F., Reach W. T., 2007, *ApJ*, 662, 544
- Wang Y.-M., Robertson J. A., 1985, *A&A*, 151, 361
- Wang Z., Chakrabarty D., Kaplan D. L., 2006, *Nature*, 440, 772
- Warner B., 1995, *Cambridge Astrophysics Series*, 28
- Webbink R. F., 1984, *ApJ*, 277, 355
- Weber E. J., Davis Jr. L., 1967, *ApJ*, 148, 217

- Wickramasinghe D. T., Ferrario L., 2000, *PASP*, 112, 873
Wickramasinghe D. T., Ferrario L., 2005, *MNRAS*, 356,
1576
Yoon S.-C., Podsiadlowski P., Rosswog S., 2007, *MNRAS*,
380, 933